

STRESS ANALYSIS USING ELASTICALLY HOMOGENEOUS RIGID-BODY-SPRING NETWORKS

John BOLANDER Jr.¹, Kenji YOSHITAKE² and Jeffrey THOMURE³

¹ Member of JSCE, Ph.D., Asst. Professor, Civil & Environmental Engrg., Univ. of California, Davis
(One Shields Avenue, University of California, Davis, California 95616-5294, USA)

² Member of JSCE, M.S.E., Research Engineer, Institute of Technology, Shimizu Corporation
(3-4-17 Etchujima, Koto-ku, Tokyo 135-8530, Japan)

³ B.S.E., Graduate Student, Civil & Environmental Engrg., University of California, Davis
(One Shields Avenue, University of California, Davis, California 95616-5294, USA)

A method is introduced for extracting tensorial stress measures from rigid-body-spring networks with random geometry. Stress analysis of a uniformly stretched material indicates that rigid-body-spring networks can be made elastically homogeneous provided two basic conditions are met: 1) network geometry is defined by a Voronoi diagram, and 2) the network degrees of freedom are defined at the Voronoi cell nuclei. For more general loadings, accuracy of the stress retrieval algorithm is demonstrated through comparisons with finite element analysis results, where the finite element mesh is based on the corresponding Delaunay triangulation of the domain.

Key Words: Rigid-Body-Spring Model, stress analysis, Voronoi diagram, structural analysis

1. INTRODUCTION

Lattice networks have been used to analyze fracture in various natural and engineered materials¹. Typically, these networks are formed from simple mechanical elements, such as central force springs or beam-springs, which are interconnected at nodal sites. Material disorder is modeled by assigning different properties to the lattice elements, either in direct relation to material structure or according to some statistical description of the material. When modeling cement-based composites, for example, the lattice elements can be associated with the mesoscopic components of the material (i.e. mortar matrix, aggregate inclusions, and matrix-inclusion interfacial zones)².

Most modeling applications have involved lattice networks with regular geometry. Regular networks, however, strongly bias the directions of potential crack propagation. Lattices constructed using randomly distributed nodal sites can greatly reduce such mesh bias, although they are not elastically homogeneous under uniform straining³. That is, random geometry networks may exhibit highly nonuniform local deforma-

tions during uniform straining of the macro-continuum.

The rigid-body-spring model (RBSM) approach, developed by Kawai⁴, is illustrated in **Fig. 1** for the two-dimensional case. The domain is partitioned into a collection of rigid convex polygons, or cells. In anticipation of the work which follows, a Voronoi diagram⁵ has been used to define the cell geometries. The cells are interconnected along their boundaries through spring sets, each of which consists of a normal, tangential, and rotational spring oriented local to the boundary segment. Cell degrees of freedom are defined at some point within the cell, typically the area centroid. Details concerning the formulation of the system equilibrium equations are presented by Kawai⁴ and are not repeated here.

Bolander and Saito note that the basic elemental unit of the RBSM (i.e., the two-cell subassembly shown in **Fig. 1**) can be regarded as a special type of beam-spring element⁶. The Kawai RBSM is therefore closely related to the aforementioned lattice models, especially when regular or random mesh designs are used to finely discretize the material domain. Categorizing

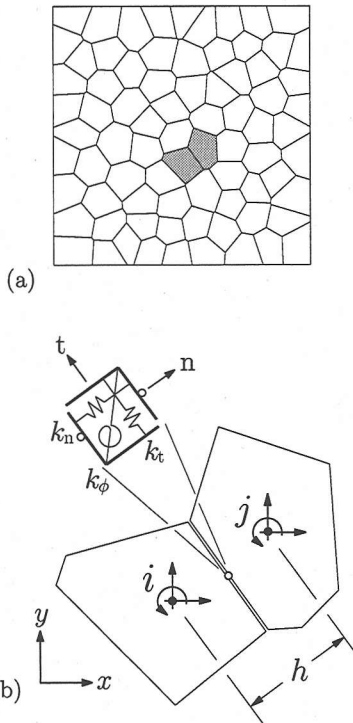


Fig. 1 Rigid-Body-Spring Model: a) partitioning of domain using a Voronoi diagram; b) elemental unit

the RBSM as a lattice model serves to unify research performed in such diverse fields as civil engineering^{2),6)} and theoretical physics¹⁾.

This article presents a novel technique for computing tensorial stress measures within rigid-body-spring networks with random geometry. Accurate stress measures are important for:

- studying the properties of the network for various load and displacement boundary conditions;
- developing fracture criteria which are invariant with respect to mesh geometry; and
- supporting various activities within structural analysis and design, such as load path visualization.

The stress retrieval algorithm is used to show that, for certain parameter settings and with proper network design, the RBSM is elastically homogeneous under uniform straining. To study model performance under more general loadings, stress analyses are performed local to a beam prestressing anchorage. Stress contours produced by the model are nearly identical to

those obtained from corresponding finite element models composed of constant strain triangle (CST) elements.

2. NETWORK DESIGN

As mentioned above, one main concern with random geometry lattices has been their inability to model a uniform strain field. Schlangen and Garboczi³⁾ studied the performance of random geometry beam lattices and developed an iterative procedure that modifies beam element cross-sectional properties to achieve elastic homogeneity for uniform stretching of the lattice network. More recently, elastic homogeneity during isotropic stretching has been achieved using the RBSM, provided: 1) a Voronoi diagram is used to partition the domain and assign spring stiffnesses, and 2) the network degrees of freedom are defined at the Voronoi cell nuclei⁶⁾. As will be shown in Section 4(1), these two aspects of the network design strongly affect the accuracy of stress measures retrieved from the network. Since network design is central to obtaining accurate results, we refer to this approach as a rigid-body-spring (RBS) network.

The link between RBS network performance and Voronoi diagrams can be partially explained as follows. For a Voronoi partitioning of a material domain under uniform straining, Jagota and Bennis⁷⁾ have derived two discrete expressions for the elastic energy stored in the continuum: one based on the continuum governing equations and the other based on a corresponding beam spring network. The beam springs are assumed to have negligible rotational stiffness. A comparison of the two expressions shows that, to model a homogeneous continuum, the beam spring constants should scale according to l/h , where l is the length of the boundary segment between contiguous Voronoi cells and h is the distance between the corresponding cell nuclei (Fig. 1). This same scaling is used for the normal and tangential springs in the RBS network, according to the RBSM approach:⁴⁾

$$\begin{aligned} k_n &= E'tl/h \\ k_t &= E''tl/h \\ k_\phi &= k_n l^2/12 \end{aligned} \quad (1)$$

where for plane stress $E' = E/(1 - \nu^2)$ and

$E'' = E/(1 + \nu)$; E and ν are the elastic modulus and Poisson ratio of the continuum material, respectively; t is the specimen thickness. Note that, in general, such explicit relationships between the network spring constants and the continuum properties are approximate.

(1) Voronoi diagram partitioning of domain

The Kawai RBSM is general in that any set of convex polytopes can be used to partition the material domain. This enables Voronoi diagram partitioning of the domain to explicitly model quasi-random aspects of the material structure (i.e., to associate the Voronoi cells with material features, such as crystal or grain boundaries)^{8),9)}. Some applications have used the Voronoi diagram in connection with modeling homogeneous continua, where the main goal is to reduce the subjective influence of mesh design on the fracture process^{6),10)}. To better understand the elastic properties of the RBS network, and the significance of network design, this article considers the modeling of homogeneous materials.

The Voronoi diagrams used here are produced from a set of randomly distributed points, or nuclei. Typically, the network nodes defining the system degrees of freedom are positioned at the area centroids of the Voronoi cells. As previously mentioned, however, there are definite advantages to positioning the network nodes at the cell nuclei. For example, elastic homogeneity of the network has been demonstrated by comparing elemental strains caused by hydrostatic straining of the macro-continuum⁶⁾. Under hydrostatic straining, only the normal (n-axis in Fig. 1) components of displacement are mobilized. The stress retrieval algorithm presented here is a means for testing network performance under more general loading conditions, including those which activate the tangential (t-axis) components of displacement.

(2) Saturated nuclei distributions

Although cell nuclei are located using a pseudo-random number generator, local regularity of the mesh design can be partially controlled by: 1) maintaining a minimum allowable distance between nuclei, d_m ; and 2) saturating the domain with nuclei. Saturated domains provide more regularity (i.e., less statistical variance in the angles formed at the Voronoi diagram triple

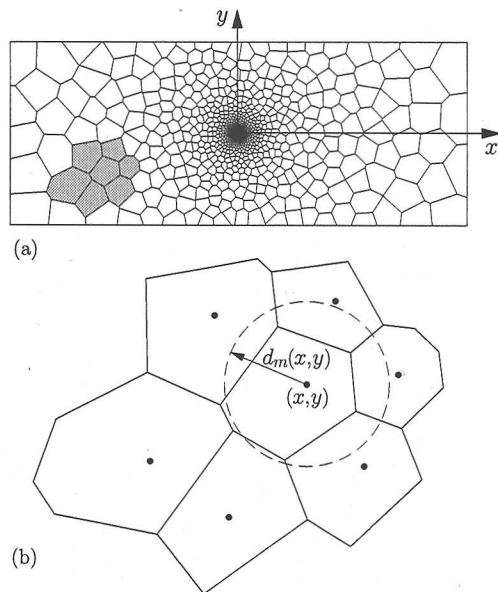


Fig. 2 Average cell size gradation

junctions), which provides greater isotropy with respect to potential cracking directions⁶⁾.

Making d_m a function of position in the domain, while maintaining local saturation, is an effective means for controlling average cell density. For example, the following relation was used to produce the cell size gradation shown in Fig. 2.

$$d_m(x, y) = \beta \sqrt{x^2 + y^2} \quad (2)$$

where β controls the rate of change in d_m with respect to distance from the origin.

3. STRESS RETRIEVAL ALGORITHM

Schlangen¹¹⁾ computes stress measures at the nodal sites of a beam lattice, rather than in the beams themselves. This article follows a similar, yet different, approach for computing stresses in a RBS network. Consider a Voronoi cell subjected to intercell spring forces, F_{ni} and F_{ti} , on each boundary segment i (Fig. 3). These are the forces in the normal and tangential springs shown in Fig. 1, according to the RBSM approach. Stress is computed by sectioning the Voronoi cell through its nodal point and then invoking force equilibrium on either portion of the cell. Although moments may also act on the cell boundary segments, moment equilibrium is not considered here. With reference to Fig. 3, the

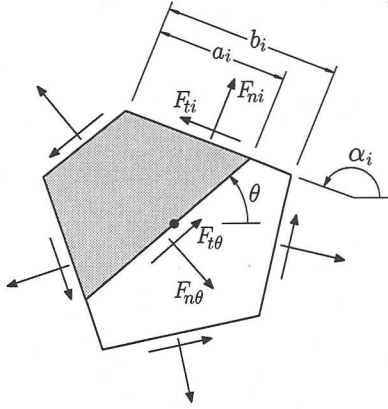


Fig. 3 Force resultants acting on a section through the cell nodal point

normal and tangential forces acting on a cut plane through the cell nodal point are¹²⁾

$$F_{n\theta} = \sum_i^N R_i [F_{ni} \cos(\pi - \alpha_i + \theta) + F_{ti} \sin(\alpha_i - \theta)] \quad (3)$$

$$F_{t\theta} = \sum_i^N R_i [F_{ni} \sin(\pi - \alpha_i - \theta) + F_{ti} \cos(\alpha_i + \theta)] \quad (4)$$

where N is the number of cell boundary segments. $R_i = a_i/b_i$ when boundary segment i intersects the cut plane; otherwise, R_i equals 1 or 0 depending on whether boundary segment i is entirely above or entirely below the cut plane, respectively. The normal and tangential stresses acting over the cut plane are

$$\sigma_\theta = F_{n\theta}/A_\theta \quad (5)$$

$$\tau_\theta = F_{t\theta}/A_\theta \quad (6)$$

where A_θ is the area of cross-sectional cut. As shown in section 4(1), the $(\sigma_\theta, \tau_\theta)$ pairs produced by varying θ from 0 to π form a Mohr's circle representation of the stress state at the cell nodal point.

Since stresses are computed at the nodal points of the RBS network, contour algorithms which operate on a triangulation of the domain can be used directly, without any need for modifying the stress values. For the finite element analyses presented later, stresses are computed within the CST finite elements and an averaging procedure is required for determining the nodal stresses used for contour plotting.

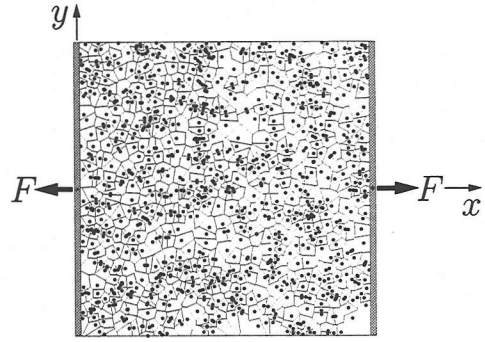


Fig. 4 Membrane subjected to uniaxial tension (cell nuclei indicated by \bullet)

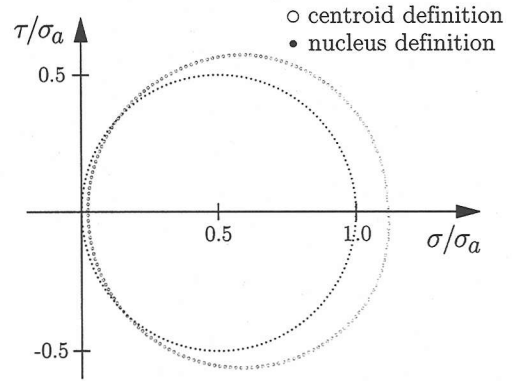


Fig. 5 $(\sigma_\theta, \tau_\theta)$ trace for a typical cell

4. STRESS ANALYSIS

(1) Membrane under uniaxial tension

Figure 4 shows a membrane structure, comprised of 1000 Voronoi cells, loaded in uniaxial tension. We have set $\nu = 0$, so that $E' = E'' = E$ in eqs. (1); other values for ν are considered later. The tangential springs are removed from the spring sets associated with the rectangular end blocks, so as not to restrict Poisson contraction of the membrane.

For a typical cell, **Fig. 5** shows the trace of $(\sigma_\theta, \tau_\theta)$ provided by eqs. (3) through (6) for θ ranging from 0 to π in increments of $\pi/180$. The normalizing factor, σ_a , is the theoretical uniaxial stress acting at any point in the membrane (i.e., $\sigma_a = \epsilon E$ where ϵ is the uniaxial strain imposed on the continuum). Location of the cell nodal point affects the accuracy of the stress measures. If the

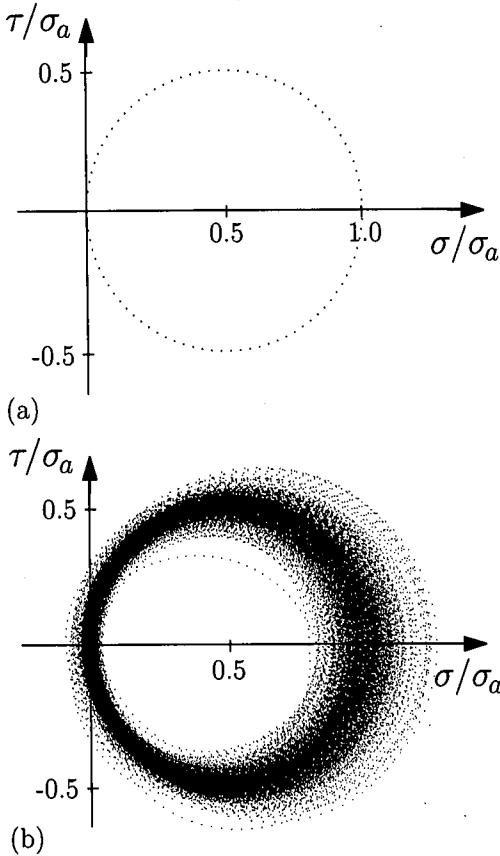


Fig. 6 $(\sigma_\theta, \tau_\theta)$ traces for network nodes defined at: a) cell nucleus; and b) cell area centroid

Voronoi cell nuclei are used, the Mohr's circle representation of stress is recovered accurately. In this case, the stress state can be determined by evaluating eqs. (3) through (6) for any two angles θ and $\theta + \pi/2$. When the nodal points are positioned at the cell area centroids, however, the trace of $(\sigma_\theta, \tau_\theta)$ deviates significantly from Mohr circle theory.

Figure 6 shows the trace of $(\sigma_\theta, \tau_\theta)$ for all 1000 cells within the membrane structure shown in **Fig. 4**. Again, the calculated stresses are accurate when the network nodes are positioned at the cell nuclei. All 1000 results match to within algorithmic precision and are indistinguishable on the plot (**Fig 6a**). In contrast, there is significant scatter in the stress measures when the network nodes are positioned at the cell area centroids (**Fig 6b**). The statistics for normal stress σ_x , corresponding to $\theta = 90^\circ$, are summarized in **Table 1**. Note that almost no restriction has been placed on the minimum

Table 1 Effect of nodal point definition on normalized stress σ_x/σ_a for $\nu = 0$

σ_x/σ_a	centroid definition	nucleus definition
mean value	1.0009	1.00000002
standard deviation	0.0662	0.0000007
minimum value	0.792	0.999992
maximum value	1.259	1.000014

Table 2 Effect of ν on normalized stress σ_x/σ_a

σ_x/σ_a	ν		
	0.1	0.2	0.3
mean value	0.9859	0.9889	1.0104
standard deviation	0.0082	0.0175	0.0289
minimum value	0.955	0.925	0.908
maximum value	1.012	1.048	1.111

allowable distance between nuclei (i.e., $d_m(x, y) \approx 0$) to accentuate the differences between the nucleus and area centroid locations. As the domains become more saturated, the nuclei and area centroids move closer together causing the scatter associated with centroid use to diminish.

As mentioned above, use of a random geometry spring network generally precludes explicit control over the effective elastic properties of the continuum. For the RBS network, setting $\nu = 0$ is special in that both E and ν are exactly realized at the continuum level. **Table 2** shows σ_x/σ_a statistics for several different ν values. Although the RBS network is not elastically homogeneous in the strict sense, the scatter in $(\sigma_\theta, \tau_\theta)$ plots for the nonzero ν values is much less than that shown in **Fig. 6b**. The modeling of the general case where $\nu \neq 0$ requires further attention, since many practical problems are strongly influenced by Poisson ratio effects.

(2) Beam prestressing anchorage

Stress analysis can be especially useful when designs are complicated by the presence of static or geometrical discontinuities. Stress analysis local to a beam prestressing anchorage (**Fig. 7**) is used to demonstrate accuracy of the stress retrieval algorithm for more general loadings. The prestressing tendon is rigidly anchored to an external block and is unbonded elsewhere. Details concerning the modeling of reinforcing components within the RBS network are given elsewhere⁶.

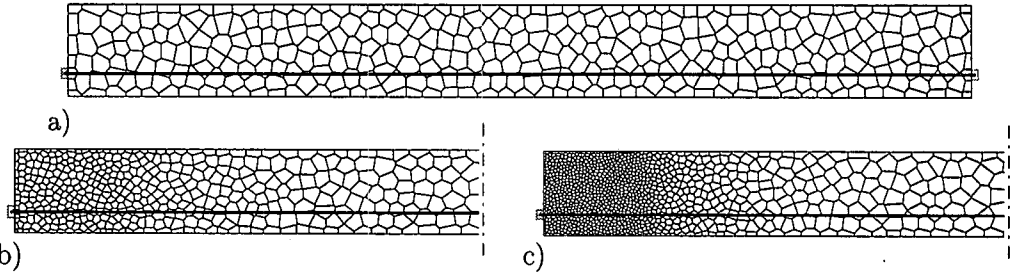


Fig. 7 Eccentrically prestressed beam modeled by a spring network with: a) constant average cell size; b) 0.4:1 average cell size ratio; and c) 0.2:1 average cell size ratio

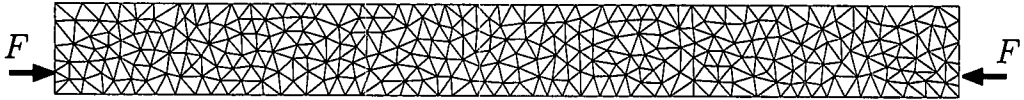


Fig. 8 Beam under eccentric axial load modeled by CST finite elements

The first RBS network shown in Fig. 7 has an average local cell density that is constant over the entire beam span. This same density is used over the central portions of the latter two networks, although higher cell densities are used local to the prestressing anchorage to obtain more accurate stress measures in that region. The ratios of average cell size near the anchorage to that used over the central portion of the span are 1:1, 0.4:1, and 0.2:1 for the three respective networks.

Beam-column theory and finite element analyses are used to assess the accuracy of the stresses extracted from these RBS networks. The mesh of CST finite elements, shown in Fig. 8, is based on the Delaunay triangulation of the set of nuclei used to construct the Voronoi diagram in Fig. 7a. The finite element and RBS network geometries are therefore uniquely associated. Note that prior to random filling of the domain, nuclei have been randomly placed very close to the domain boundaries so that the Delaunay triangulation nearly covers the rectangular domain. Finite element meshes corresponding to the other two RBS networks given in Fig. 7 are also constructed and used in the comparisons that follow. The effective prestressing force, F , is applied externally at the same location, and with the same local pressure distribution, as for the tendon anchorage blocks used in the corresponding RBS network model.

Figure 9 compares trajectories of σ_x/σ_F provided by the RBS network and finite element models loaded only with effective prestressing force, F . Here, σ_x is the normal stress acting

on the beam cross-section and $\sigma_F = F/A$ is the average axial stress in the beam with cross-sectional area A . The cell nuclei definition of the nodal points has been used here and for the analyses that follow.

Away from the anchorage zone, stress varies almost linearly over the cross-section; the contours are nearly in-line with calculations based on ordinary (i.e. first-order) beam-column theory, which are shown by the broken lines in each of the lowermost contours in the figure. With greater mesh refinement local to the anchorage, the stress contours provided by the two methods become nearly identical. This similarity is also apparent in Fig. 10, which shows contours of normalized transverse stress, σ_y/σ_F , over an enlarged view of the anchorage zone. Only the results from the fine mesh (i.e. 0.2:1 average cell size ratio) are given here, since the coarser meshes provide comparisons of similar quality to those given in Fig. 9. Contours at exactly zero stress are not plotted since they tend to emphasize small variations in the solution over the portions of the domain with near zero stress.

5. CONCLUSION

Random geometry lattices are advantageous in that they reduce network bias on potential cracking directions and offer an effective means for grading network component density. The ability to compute tensorial stress measures within the RBS network is quite significant for:

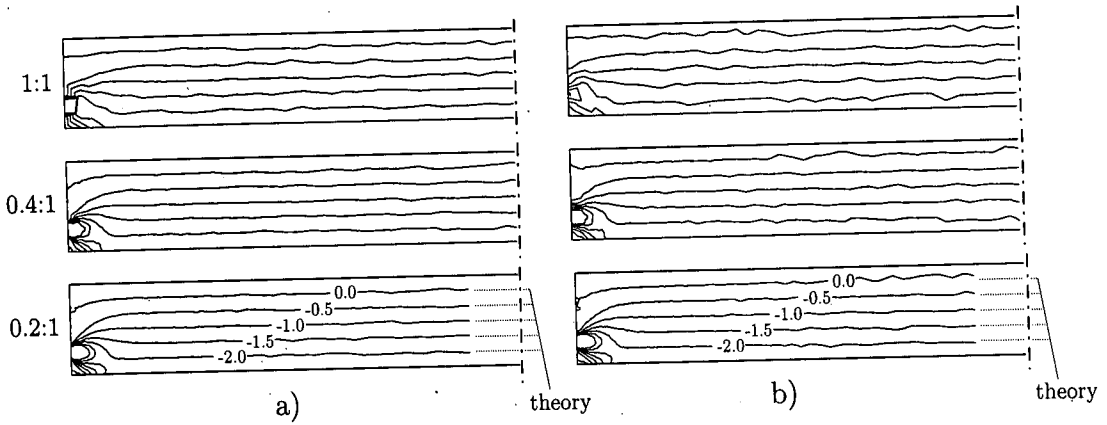


Fig. 9 Contours of σ_x/σ_F provided by: a) RBS network; b) CST finite elements

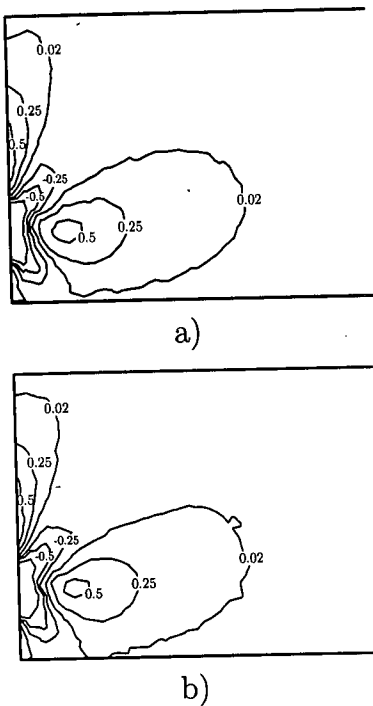


Fig. 10 Contours of σ_y/σ_F provided by: a) RBS network; b) CST finite elements

1) assessing the properties of the RBS network itself, 2) developing more general and effective fracture criteria, and 3) promoting the RBS network methodology as a structural design tool.

This article presents a novel method for extracting tensorial stress measures from RBS networks with random geometry. Previous work⁶⁾ has shown that the Kawai RBSM can be used to construct an elastically homogeneous material description with respect to hydrostatic straining,

provided: 1) the model geometry is defined using a Voronoi diagram, and 2) the Voronoi cell nuclei are used to define the model degrees of freedom. Stress computations performed here confirm that networks which satisfy these two criteria can also be made elastically homogeneous for uniaxial straining of the macro-continuum. This is noteworthy because, unlike hydrostatic straining, uniaxial straining activates both the normal and tangential degrees of freedom defined local to the cell boundary segments. In this sense, uniaxial straining is a more rigorous test of the network's abilities to model a homogeneous continuum.

The accuracy of stresses calculated for more general loading conditions has been verified by comparisons with results from finite element analyses. Stress analyses near a beam prestressing anchorage have been presented as an illustrative example. By basing the finite element mesh on the Delaunay triangulation of the network nodal sites, a unique correspondence between the two models is maintained for different mesh densities and gradations. These comparisons indicate the stress measures extracted from RBS network models are comparable in accuracy to those from CST finite elements. Additional work is needed to determine the applicability of the approach when Poisson ratio effects are large.

ACKNOWLEDGMENTS: The previous contributions to this work of Mr. Shigehiko Saito at Kyushu University, Fukuoka, Japan, and Dr. Gi-Suop Hong at Hong-Ik University, Seoul, Korea, are gratefully acknowledged.

REFERENCES

- 1) *Statistical Models for the Fracture of Disordered Media*, Herrmann, H.J. and Roux, S. eds., Elsevier/North Holland, Amsterdam, 1990.
- 2) Schlangen, E. and van Mier, J.G.M.: Experimental and numerical analysis of micromechanisms of fracture of cement-based composites, *Cem. Conc. Composites*, Vol. 14, pp. 105-118, 1992.
- 3) Schlangen, E. and Garboczi, E.J.: New method for simulating fracture using an elastically uniform random geometry lattice, *Int. J. Engng. Sci.*, Vol. 34, No. 10, pp. 1131-1144, 1996.
- 4) Kawai, T.: New discrete models and their application to seismic response analysis of structures, *Nuclear Engng. Design*, Vol. 48, pp. 207-229, 1978.
- 5) Preparata, F.P. and Shamos, M.I.: *Computational Geometry - An Introduction*, Springer-Verlag New York Inc., 1985.
- 6) Bolander, J.E. and Saito, S.: Fracture analysis using spring networks with random geometry, *Engng. Fracture Mech.*, Vol. 61, No. 5-6, pp. 569-591, 1998.
- 7) Jagota, A. and Bennison, S.J.: Spring-network and finite element models for elasticity and fracture. In *Nonlinearity and Breakdown in Soft Condensed Matter* (Springer Lecture Notes in Physics 437) eds. K.K. Bardhan, B.K. Chakrabarti, and A. Hansen, Springer-Verlag, Berlin, 1994, pp. 186-201.
- 8) Toi, Y. and Che, J.-S.: Mesoscopic simulation of microcracking behaviors of brittle polycrystalline solids, *Proc. Japanese Soc. of Mechanical Engineers*, Vol. 59, No. 557, pp. 240-247, 1993. (in Japanese)
- 9) Toi, Y. and Kiyosue, T.: Three-dimensional meso-mechanical analysis of brittle solids containing microinclusions, *Proceedings Japanese Society of Mechanical Engineers*, Vol. 61, No. 582, pp. 237-243, 1995. (in Japanese)
- 10) Ueda, M., Kambayashi, A., Kitoh, H. and Takeuchi, N.: Size effect analysis using RBSM with Voronoi elements, in *Size Effect in Concrete Structures*, Mihashi, H., Okamura, H. and Bazant, Z.P. eds., E & FN Spon, pp. 221-232, 1994.
- 11) Schlangen, E.: Computational aspects of fracture simulations with lattice models, *Fracture Mechanics of Concrete Structures*, Wittmann, F.H. ed., Aedificatio Publ., Freiburg, Germany, pp. 913-928, 1995.
- 12) Bolander, J.E.: Stress analysis using random geometry spring networks, *Engineering Mechanics: A Force for the 21st Century*, 12th Engineering Mechanics Division Conference, Luco, J.E. and Murakami, H. eds., ASCE, pp. 630-633, 1998.

(Received May 12, 1999)

弾性的に均質な剛体一ばねモデルによる応力解析

John BOLANDER · 吉武謙二 · Jeffrey THOMURE

有限要素解析における要素内の応力がテンソル量であるのに対し、剛体一ばねモデル解析で求められる応力は要素境界辺における表面力（ベクトル量）である。本論文では、ランダム形状要素を用いた剛体一ばね系モデルに基づく応力テンソルの解析法を提案する。まず、一様な引張りを受ける材料の応力解析から、剛体一ばね系は次の2つの条件を満たすとき弾性的に均質であることを示す。すなわち、1) 剛体要素の幾何形状がヴォロノイ分割図で定義されること、および2) 系の変形自由度がヴォロノイ分割の母点で定義されること。さらに、より一般的な荷重条件に対して、この応力テンソル算定アルゴリズムの適用性と精度を有限要素解析結果との比較により提示する。